Femtosecond Spectroscopy of Calcium Dipicolinate - A Major Component of Bacterial Spores

SUPPORTING INFORMATION

Ramona Mundt[1,#], Christian Torres Ziegenbein[1,#], Sascha Fröbel[1], Oliver Weingart[2], and Peter Gilch[1,*]

August 29, 2016

1 Quantum mechanical calculations

The SI provides detailed geometry and TDDFT benchmark data for excited state geometry optimizations of CaDPA in implicit aqueous solution.

1.1 TDDFT Optimizations

In many cases the DFT-MRCI method delivers accurate results for excitation energies, but analytic gradients to perform structure optimizations are not available. Producing reliable excited state structures generally constitutes a major challenge, especially when solvent effects are included and no experimental excited state structure parameters are available. Correlated methods like, e.g. the CASSCF/CASPT2 approach, require large orbital spaces and are therefore too demanding for optimizing the CaDPA geometry. To evaluate the performance of DFT and TD-DFT optimization techniques for CaDPA, different functionals were tested to obtain ground and excited structures. Mennucci and co-workers[1] suggest to perform excited state TD-DFT optimizations with the CAM-B3LYP rather than the common B3LYP functional in order to include the long range electrostatic effects resulting from the solvent. Consequently, we tested these two approaches. The BH-LYP functional forms the basis for the parameterization of the DFT-MRCI-method and is therefore included and also tested against the B3LYP methods. All optimizations were carried out with the Gaussian program suite, applying the 6-31++G** basis set for the CAM-B3LYP methods. The basis set TZVP, i.e. the very same basis as used for excited state property computations with DFT-MRCI, was employed for BH-LYP. For each functional, the TD-DFT geometry-optimized structures were compared with respect to their excitation energies with the DFT-MRCI results. We begin with a comparison of the vertical excitation energies after ground state optimization. Table S1 collects the values for the first bright $\pi\pi^*$ state and the two lowest $n\pi^*$ states.

Considering the experimental value of 4.59 eV, all DFT methods largely overestimate the vertical excitation energy and generate two low lying and closely spaced $n\pi^*$ states. B3LYP shows the largest $\pi\pi^*$ - $n\pi^*$ splitting, as it places the bright excitation

Table S 1: Vertical excitation energies for the first bright $\pi \rightarrow \pi^*$ state and the lowest two $n \rightarrow \pi^*$ states for DFT optimized ground state geometries with various functionals.

Method	DFT State	vert. exc.[eV]	f	DFT-MRCI exc. [eV]	Energy	Exc. Type
B3LYP	S_7	5.03	0.1542	4.78	-1301.743608	$\pi \rightarrow \pi^*$
	S_2	4.22	0.0002	4.72	-1301.745690	$n \rightarrow \pi^*$
	S_1	4.20	0.0000	4.70	-1301.746359	$n \rightarrow \pi^*$
	S_0	-	-	-	-1301.919067	
BH-LYP	S_3	5.50	0.1492	4.94	-1301.732927	$\pi \rightarrow \pi^*$
	S_2	5.27	0.0000	4.86	-1301.735332	$n \rightarrow \pi^*$
	S_1	5.19	0.0013	4.82	-1301.737060	$n \rightarrow \pi^*$
	S_0	-	-	-	-1301.914282	
CAM-B3LYP	S_3	5.18	0.2483	4.86	-1301.742502	$\pi \rightarrow \pi^*$
	S_2	4.82	0.0000	4.78	-1301.745094	$n \rightarrow \pi^*$
	S_1	4.79	0.0010	4.54	-1301.746043	$n \rightarrow \pi^*$
	S_0	-	-	-	**-1301.920946**	

into the S_7 state. In the DFT-MRCI computation, the B3LYP geometry yields the S_3 excitation energy closest to the experiment. The $n\pi^*$ states are only 0.06 eV apart from the bright excitation. The CAM-B3LYP geometry delivers the lowest absolute DFT-MRCI energy for the S_0 state (bold faced value in Table S1).

Table S2 collects the computed excitation energies with reference to the geometry of the bright state. In this computation, B3LYP and CAM-B3LYP place the bright $\pi\pi^*$ excitation above the $n\pi^*$ states, whereas BH-LYP computes it as the lowest excited state. In DFT-MRCI, the bright excitation stays above the $n\pi^*$ states for the B3LYP geometry, while BH-LYP and CAM-B3LYP geometries yield a low lying $\pi\pi^*$ state (marked as bold face in the table). Again, the lowest absolute DFT-MRCI energy for this state is obtained with CAM-B3LYP, i.e. the CAM-B3LYP generated structures are obviously closer to a potentially DFT-MRCI optimized geometry. Figure S1 denotes the differences in bond lengths in the used approaches, with B3LYP yielding the largest deviation for the optimized bright state geometry. The tests indicate that CAM-B3LYP delivers, with respect to the DFT-MRCI results, the most valuable description among the tested functionals, it was therefore used for all ground and excited state geometry optimizations.

Table S 2: Vertical excitation energies for the same states as in Table S1, but using the optimized bright state TD-DFT geometries as starting points. The '*' marks the bright $\pi \rightarrow \pi^*$ state in the corresponding description. The other states are due to $n \rightarrow \pi^*$ excitation.

Method	State	DFT exc. [eV]	f	DFT-MRCI exc. [eV]	Energy
B3LYP	S_7	4.40*	0.1738	4.42* (S_3)	-1301.739122*
	S_2	3.65	0.0001	4.22	-1301.746490
	S_1	3.56	0.0000	4.18	-1301.748071
	S_0	-	-	-	-1301.901513
BH-LYP	S_3	5.06*	0.2734	4.69	-1301.736262
	S_2	5.09	0.0013	4.68	-1301.736600
	S_1	5.12	0.0000	**4.54***	-1301.741632*
	S_0	-	-	-	-1301.908603
CAM-B3LYP	S_3	4.81*	0.2679	4.60	-1301.743564
	S_2	4.64	0.0005	4.58	-1301.744309
	S_1	4.64	0.0000	**4.47***	**-1301.748406***
	S_0	-	-	-	-1301.912656

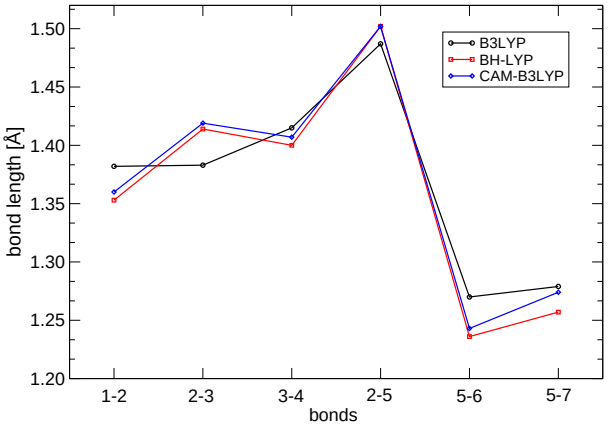

Figure S 1: Bond lengths in optimized $\pi\pi^*$ state structures computed with various functionals.

1.2 Geometry parameters

Geometry parameters for (TD)CAM-B3LYP optimized structures are collected in Table S3. The atom numbering is given in Figure S2. Upon excitation to the bright S_3 state, all aromatic ring bonds elongate. This is also true for the S_1 and S_2 structures.

Larger changes in bond angles can be observed for the C_s symmetric T_1 structure. The additional column (T_1') denotes the corresponding asymmetric bonds (primed numbers in Figure S2) in this geometry, which differ by up to 0.07 Å. An overlay of the most relevant structures is shown in Figure S3.

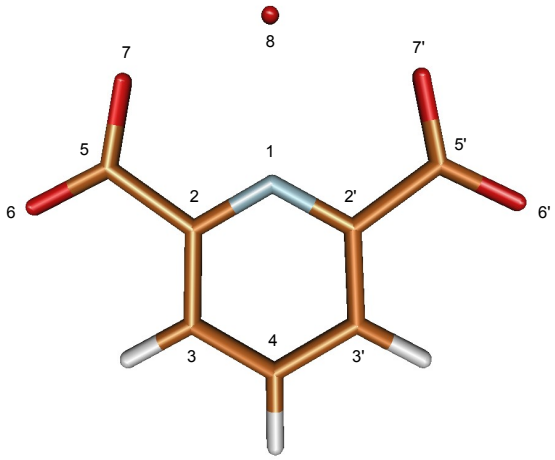

Figure S 2: Atom numbering in CaDPA.

Table S 3: Geometry parameters of CAM-B3LYP optimized structures.

structure	S_0	S_3	S_2	S_1	T_1	T_1'
bonds (Å)						
1-2	1.329	1.360	1.346	1.349	1.348	1.401
2-3	1.387	1.419	1.399	1.398	1.365	1.400
3-4	1.389	1.407	1.390	1.391	1.427	1.377
2-5	1.527	1.502	1.461	1.461	1.521	1.453
5-7	1.271	1.274	1.284	1.284	1.249	1.279
5-6	1.234	1.243	1.267	1.268	1.254	1.268
1-8	2.422	2.360	2.419	2.397	2.339	-
7-8	2.337	2.376	2.364	2.371	2.420	2.343
angles (deg)						
1-2-3	121.230	122.547	121.480	121.641	125.572	120.911
2-3-4	118.262	120.282	118.217	118.260	117.861	120.603
2-1-2´	121.207	117.647	120.253	119.897	116.527	-
1-2-5	114.590	114.295	113.556	113.539	110.600	113.164
2-5-7	114.730	114.276	118.763	119.109	118.490	118.604
2-5-6	118.246	118.727	121.572	121.338	116.926	119.075
6-5-7	127.024	126.997	119.666	119.552	124.584	122.322
5-7-8	124.730	124.046	121.402	120.445	120.583	120.888
7-8-7´	133.108	132.415	132.811	133.710	134.198	-

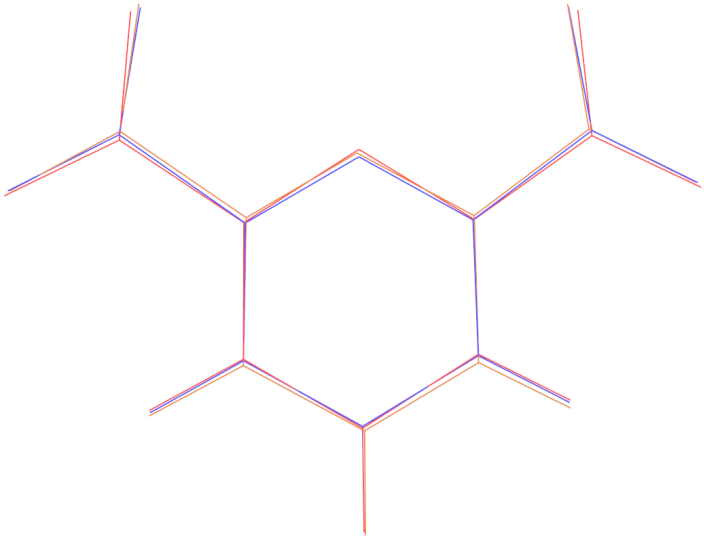

Figure S 3: Overlay of S_0 (blue), S_3 (red) and T_1 optimized structures (orange). For the computed S_1 and S_2 geometries there is no visible difference to S_3.

References

[1] Guido, C. A.; Knecht, S.; Kongsted, J.; Mennucci, B. Benchmarking Time-Dependent Density Functional Theory for Excited State Geometries of Organic Molecules in Gas-Phase and in Solution. *Journal of Chemical Theory and Computation* **2013**, *9*, 2209–2220.